KfK 3160
Oktober 1981

# New Experimental Techniques

G. Flügge
Institut für Kern- und Teilchenphysik

Kernforschungszentrum Karlsruhe

KERNFORSCHUNGSZENTRUM KARLSRUHE

Institut für Kern- und Teilchenphysik

KfK 3160

# NEW EXPERIMENTAL TECHNIQUES

G. Flügge

Invited talk at the International Conference on High Energy Physics, Lisbon, July 1981

Kernforschungszentrum Karlsruhe GmbH, Karlsruhe

Kernforschungszentrum Karlsruhe GmbH
ISSN 0303-4003

# New Experimental Techniques


## Abstract

New developments in experimental techniques for elementary particle detectors are described. Tracking devices, calorimeters, and particle identification are discussed.


# Neue Experimentelle Techniken


## Zusammenfassung

Neue Entwicklungen in den experimentellen Techniken für Elementarteilchen-Detektoren werden beschrieben. Spurennachweis, Kalorimetrie und Teilchenerkennung werden diskutiert.

# NEW EXPERIMENTAL TECHNIQUES

G. Flügge
Kernforschungszentrum and Universität Karlsruhe, Germany

## 1. Introduction

Considerable effort has been spent in the last years to meet the ever increasing demands to improve experimental techniques in high energy experiments: fixed target spectrometers asked for precise tracking and full range particle identification for charm and bottom spectroscopy, calorimeters were needed for neutrino and jet physics, vertex detectors for charm lifetime measurements, to mention only some recent developments. Even more so storage ring experiments demanded multipurpose devices incorporating all these techniques with the additional challenge to cover the full solid angle with densely packed detectors.

The purpose of this talk is to give a survey of the latest developments that have been achieved. Within the scope of this short review most topics will be touched very briefly only.

I will cover the subjects of tracking devices, calorimetry, and particle identification. Unfortunately, I will not have the time to talk about data handling. For this topic I rather refer to the parallel sessions, where many interesting contributions[1] have been presented, e.g. about the use of emulators[2] and new ideas on particle tracking[3].

## 2. Tracking Devices

For all types of tracking devices there have been developments towards high precision vertex detectors (Table 1). Since these have been covered in the previous talk[4] I will rather concentrate on another important stream of evolution in drift chamber construction: imaging drift chambers for large storage ring detectors.

Table 1: TRACKING DEVICES

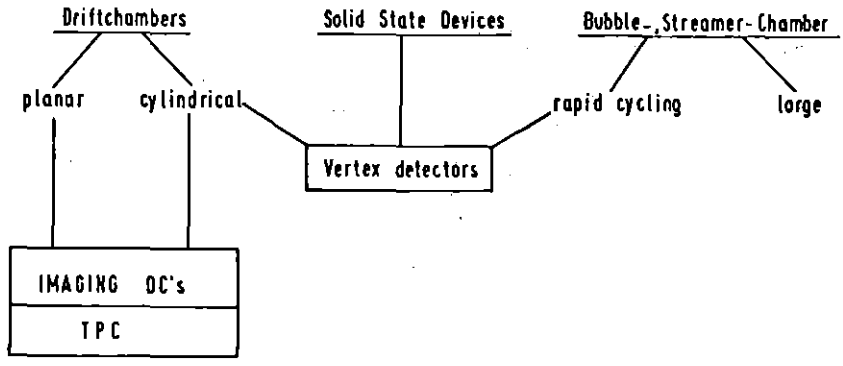


Most of the large detector systems operating or being installed at colliding beam machines (Table 2) employ solenoidal magnetic fields parallel to the stored beams for charged particle momentum analysis. An exception is the UA1 detector at the $p\bar{p}$ collider at CERN which will utilize a transverse dipole field of 0.7 T. The majority of detectors (Table 2) is equipped with copper or aluminium coils producing B-fields of about 0.5 T. The superconducting coils in use allow for fields up to 1.5 T.

Table 2: Some Magnetic Tracking Detectors at Colliding Beam Machines

| Type | Magnet | $\frac{\Delta\Omega}{4\pi}$ | | Track radial length (mm) | Track samplings | Spatial Resol. $r\phi(\sigma)$ | Spatial Resol. $z(\sigma)$ | $\sigma_p/p^2$ %·GeV$^{-1}$ | Reference |
|---|---|---|---|---|---|---|---|---|---|
| PWC cath.r.o. minimal DC small $\frac{1}{2}$ stereo | 0.5 T | .91 | DM2 | DC: 540 | 6 PWC 13 DC | 180μ | 1mm | 1.5 | 16 |
| imaging DC 4 atm | 0.45T | .97 | JADE | 600 | 48 | 180μ | 16mm | 2.2 | 5 |
| minimal DC small $\frac{1}{2}$ stereo | 0.5 T | .91 | TASSO | 855 | 15 | 220μ | 3-4mm | 2.0 | 6 |
| PWC cath.r.o. + min. DC | 1.3 T sc | .91 | CELLO | 530 | 12 $r\phi$<br>5 z<br>5 30° | 220μ | 0.4mm | 2.0 | 7 |
| min DC small $\frac{1}{2}$ stereo | 0.5 T (1.5T sc)+ | .96 | CLEO | 800 | 17 | 250μ | 5mm (0.3mm)++ | 5.0 | 8 |
| min. DC small $\frac{1}{2}$ stereo | 0.4 T | .83 | MARK II | 1034 | 16 | 200μ | 4mm | 1.9 | 9 |
| imag. DC 1 atm | 0.5 T | .92 | AFS | 600 | 42 | 250μ | 17mm | 2.5 | 10 |
| imag. DC 10 atm | 1.5 T sc | .95 | TPC | 800 | 185 dE/dx<br>15 $r\phi$ | 100μ** | ≤0.2mm** | ∼1.0* | 11,17 |
| imag. | 0.7 T Dip. | ∼1. | UA1 | 1120 | $\frac{1}{2}$ depend. | drift: 220μ<br>ch.div.: 8-25mm | | | 12 |
| minimal DC small $\frac{1}{2}$ stereo | 1.5 T sc | .92 | HRS | 1550 | 17 | 230μ | 3mm | <0.5† | 13 |

*Inferred from space resol.
**Small test chamber
+in preparation
++beam pipe PWC's
†∼.25 for 17 samplings expected

The elevated B-field of superconducting magnets facilitates a more compact tracking detector for a given momentum resolution. Moreover novel designs of high current density superconducting coils[7,11] result in a considerably reduced wall thickness (typically 0.5 $X_o$ for coil, cryostat and insulating material as opposed to more than 1 $X_o$ for normally conducting coils) and thus interfere to a much lesser extent with the detection of low energy photons and electrons in electromagnetic calorimeters outside the coil.

Magnetic field volumes are such, that radial track lengths vary between 0.5 m and over 1 m. The solid angle coverage usually exceeds $0.9 \times 4\pi$.

Whereas in the first generation of magnetic detectors at $e^+e^-$-storage rings (MARK I at SPEAR and PLUTO at DORIS and PETRA) cylindrical spark or proportional wire chambers were used, charged particle tracking nowadays primarily relies on cylindrical drift chambers. There are two basic concepts.

Minimal drift chambers:

In these chambers the number of potential wires is kept to a minimum. Drift cells are arranged on cylindrical surfaces. Adjacent sense wires are separated electrostatically by a triplet of potential wires (DM2 and ARGUS have further shape und shield wires). There are no further field shaping electrodes. Minimal drift chambers which were first used in the MARK II detector at SPEAR have been applied in many magnetic tracking detectors (Table 2) and will be used in the new detector ARGUS[15] at DORIS and the new PLUTO inner detector. MARK III[14] at SPEAR uses a combination of minimal and imaging drift chambers.

Imaging drift chambers:

They record charged particle trajectories by sampling three dimensional space points along the ionization track. The measurement of correlated coordinates is particularly useful to reconstruct events with high track density like high multiplicity jet events. Examples of imaging drift chambers are the inner detectors of JADE[5] at PETRA, and AFS[10] at the ISR. The cylindrical chamber volume is

subdivided into azimuthal sectors by cathode planes. In the median plane of each sector alternating sense and potential wires are strung parallel to the detector and B-field axis. Each sense wire determines a space point $(r,\phi,z)$ by its position (r), by drift time ($\phi$) and charge division (z) measurements.

A different type of imaging chamber is employed in the UA1 detector[12] at the $p\bar{p}$ collider (Fig. 1). Particle tracks are drifted between parallel cathode and anode planes. The drift direction is perpendicular (parallel) to the beam axis in the forward (central) part of the inner detector. Again the magnetic dipole field is perpendicular to the electric field.

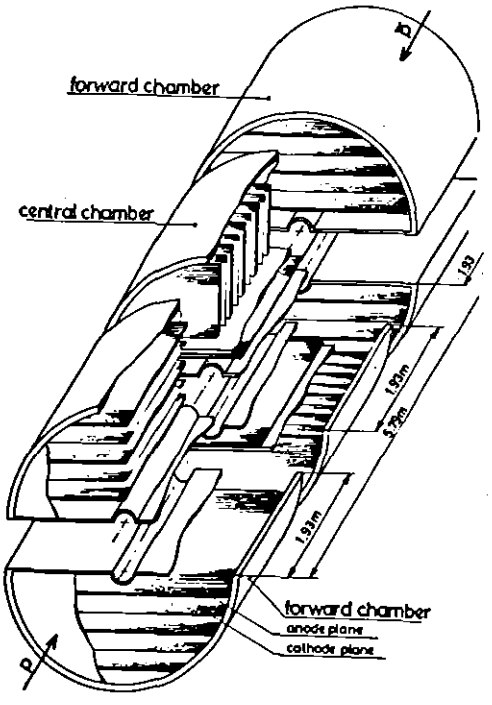


Fig. 1: Central detector of the $p\bar{p}$ collider experiment UA1 [12].

The most radical concept of an imaging drift chamber is the Time Projection Chamber (TPC) developped at Berkeley[11,17] (Fig. 2). In the TPC the electric drift field is aligned with the magnetic field ($\vec{E} \times \vec{B} = 0$). The E-field forces the ionization electrons to drift onto the chamber endcaps. There, proportional wires and cathode segments ("pads") (Fig. 2) measure the coordinates orthogonal to the drift direction z. The z coordinate is determined by the measured drift time.

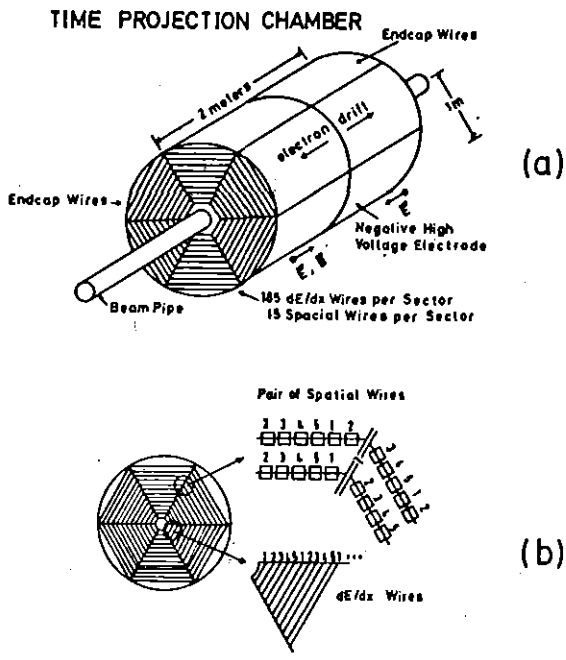


Fig. 2: The Time Projection Chamber of the PEP4-Experiment[11,17)]
(a) schematic view
(b) schematic view of read out plane consisting of PWC sectors equipped with anode wires and cathode segments ("pads").

The longitudinal B-field greatly reduces the transverse diffusion of the drifting electron swarm thus allowing for a precise position measurement in the plane of magnetic deflection ($r\phi$ plane). For the Berkeley TPC the maximum drift length is 1 m (Fig. 2a). A spatial accuracy of about 100 µm in the $r\phi$-plane is expected and was actually achieved in a small test chamber[17)].

There are up to 185 samplings per track in order to determine the particle velocity by dE/dx-measurement. To achieve sufficient dE/dx-accuracy the chamber will be operated at a gas pressure of 7 to 10 atmospheres.

The PEP-TPC has been successfully operated in cosmic ray tests.

The spatial accuracy obtained by drift time measurement ($r\phi$-determination for all detectors except TPC) is about 200 µm rms in all large systems (Table 2). This demonstrates that the substantial drift path distortion caused by the uncompensated Lorentz force of the momentum analysing B-field is well understood.

The spatial accuracy achieved in large detectors is limited by systematic uncertainties like quantization of time digitization, wire displacement due to gravitational and electrostatic forces, alignment errors and others. The inherent spatial resolution of the drift chamber types listed in table 2 as measured with small prototypes or in single cells is 100 μm or better.

In cylindrical geometry the measurement of the coordinate z along the axis poses a problem. The various techniques used to determine z are:

1) charge division measurement (JADE, AFS): though the precision is poor (15-20 mm) the method has the advantage of yielding correlated r, $\phi$ and z coordinates.
2) Small angle stereo measurement (MARK II, TASSO, CLEO): a precision of $\sigma_z = \sigma_{r\phi}/\sin\alpha \simeq 3\text{-}5$ mm is obtained.
3) Cathode readout (CELLO, CLEO): a resolution of 300 to 400 μm has been achieved in the CELLO[7] and CLEO[18] detectors using analog readout.
4) Drift time measurement (TPC). A resolution of about 400 μm is expected[17].

The momentum precision $\sigma_p/p^2$ achieved in most tracking detectors listed in table 2 is about 2% $GeV^{-1}$. Exceptions are the TPC and the HRS with anticipated accuracies of 1 and 0.5% respectively.

A promising tool to improve the spatial resolution of large drift chambers by eliminating systematic uncertainties is developping with the observation of ionization by UV laser light[19,20]. Primary ionization of more than 2000 $e^-$/cm has been observed with a high power $N_2$-laser resulting in a narrow pulse height spectrum of 9% FWHM. Ionization tracks could be localized to within 50 μm rms.

## 3. CALORIMETERS

The various types of calorimeters and their recent developments are listed in table 3.

Table 3: CALORIMETERS

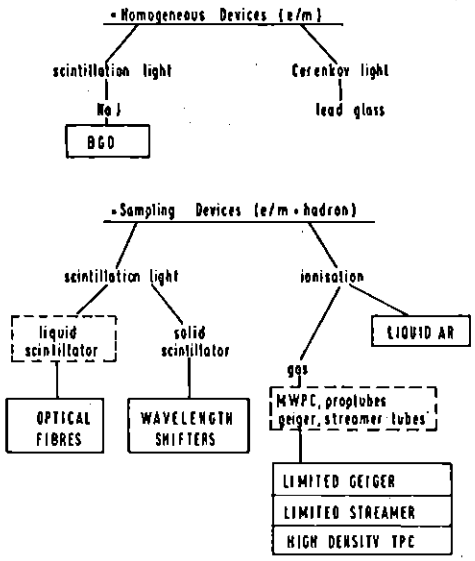


## Homogeneous Devices

Two types of homogeneous devices are commonly used for electromagnetic shower detection: NaI and leadglass. Recently, tests have been made to apply Bismuth-germanate ($Bi_4 Ge_3 O_{12}$ "BGO") in high energy shower detection[21]. Compared to NAI(Tl) it also produces scintillation light but offers several advantages

- the radiation length of 1.12 cm is much shorter than in NaI (2.56 cm)
- it is not hygroscopic
- since it is a primary scintillator, its energy response goes like $E^{-1/2}$ compared to $E^{-1/4}$ of NaI. Extrapolating from low energy measurements one may hope for a high energy resolution of better than 1%.

The present prices per $cm^3$ are of the order of 5-8 $ compared to about 1 $ for NaI. (This price difference is of course partly compensated by the shorter radiation length.)

## Sampling Devices

There exists a very large variety of sampling devices both for electromagnetic and hadron calorimetry (Table 3) using either scintillation light or ionisation in the active part.

Liquid Scintillators

Liquid scintillators offer the advantage of being cheap and easily adaptable to complicated geometries. Their disadvantage is (besides being liquid) the comparatively low density. SLIC[22], an example for a new large area (12 $m^2$) detector of this type has been presented to this conference. Its performance parameters of $\sigma_E/E = 12\%/\sqrt{E}$ and $\sigma_x \simeq 3$ mm are typical for such detectors.

Optical fibres

An appealing new development are scintillating optical fibres[23]. They consist of a scintillating core in some cladding material with lower refractive index ($n_{core} > n_{clad}$). E.g. Martin et al.[24] proposed to use liquid scintillator in a teflon tube of 5 mm Ø and 0.4 mm wall thickness. Bornstein et al.[25] proposed plastic scintillating optical fibres as core material. In test samples they measured attenuation lengths of about 2 m. The use of photodiodes in conjunction with optical fibres is being considered.

Wave length shifters

The wave length shifter technique has replaced the light guide readout of scintillators in most large calorimeters in the past few years. Examples are the NA5 calorimeter[27] with its nice two colour readout of the electromagnetic and hadron part and the large electromagnetic and hadron calorimeters of UA1 and UA2 for the $p\bar{p}$ collider. Typical resolutions are $\sigma_E/E \simeq 10\text{-}15\%/\sqrt{E}$ and $\sigma_x \simeq 1$ cm for electromagnetic showers and $\sigma_E/E \simeq 60\text{-}80\%/\sqrt{E}$ for hadrons. The problems inherent to the use of many photomultipliers (magnetic field, calibration stability) of course remain in large systems.

A speciality of the AFS spectrometer at the ISR is its fission compensated Uranium calorimeter[28]. Extensive tests showed that the fission compensation results in a very similar response for electrons and hadrons ($e/\pi$ ratio of $1.15 \pm 0.02$) which improved the hadron resolution to $35\%/\sqrt{E}$. This is consistent with an intrinsic resolution of $20\%/\sqrt{E}$ for an ideal Uranium calorimeter.

A high resolution ($7\%/\sqrt{E}$) electromagnetic calorimeter for the energy range 70 MeV to 6 GeV to be used at the ARGUS detector at DORIS was presented at this conference[29].

Possible advanced applications using double wave length shifting technique in a calorimeter have been proposed by Pretzl[30] and Palmer[23]. The light is collected and re-emitted twice in differently doped scintillator bars with $\lambda_1 < \lambda_2 < \lambda_3$ (e.g. scintillator, POPOP, BBQ).

Liquid Argon

The sampling with liquid argon ionization gaps is another technique which has found large scale application. It was nearly exclusively applied for electromagnetic shower detection using Pb. Examples for large devices can be found in storage ring detectors at PEP (MARK II), PETRA (TASSO and CELLO), and the ISR (R806) as well as at fixed target detectors at FNAL (E272, E629)[31] and the SPS (LAD)[32].

The typical resolutions are $\sigma_E/E \simeq 8\text{-}12\%/\sqrt{E}$ and $\sigma_x \simeq$ some mm. Fig. 3 shows as an example the energy resolution of the CELLO detector[7].

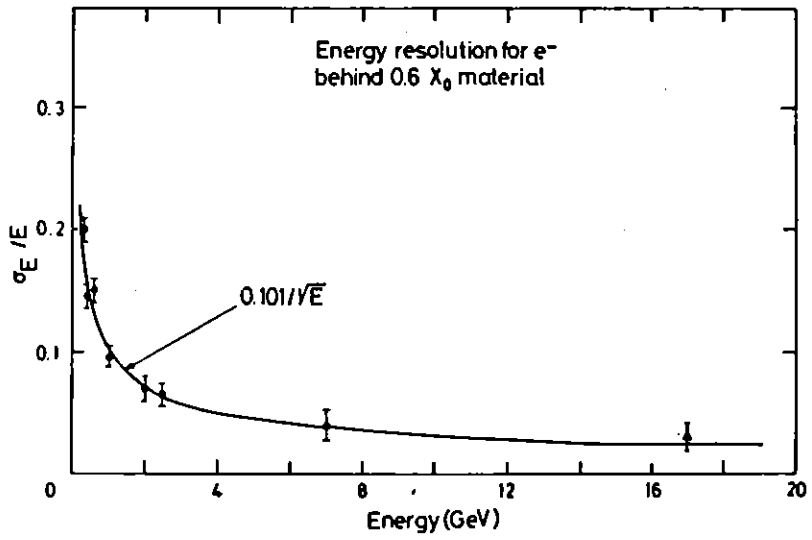


Fig. 3: Energy resolution of the CELLO Pb/LAR-calorimeter as measured in an e⁻ beam at DESY with 1 $X_0$ of passive material in front. The point at 18 GeV has been measured with Bhabha scattering at PETRA[7].

Gas sampling calorimeters

Proportional tubes and chambers have been used in sampling devices since a couple of years. Examples are the endcaps of MARK II, and the MARK III detector at SPEAR (MWPC), or the CHARM neutrino experiment at the SPS and the MAC detector at PEP (prop. tubes). This technique offers good shower location whereas the energy resolution is typically 50% worse than in comparable devices using solid or liquid detectors.

The idea to use flash tubes in large calorimeters has been put forward several years ago[33]. A large flash tube calorimeter is operated by the FMMN collaboration for neutrino physics at FNAL. These ideas were further pursued with the increasing interest in large proton decay and neutrino oscillation detectors. The advantage of the technique is of course the low price, large signal and reliability. Disadvantages are low density and saturation effects due to a relatively large cell size (low multihit resolution).

Several ideas have been proposed to reduce the effective cell size:

- Limited streamer: tubes are operated in the limited streamer mode by using an appropriate quenching gas[34]. This method in conjunction with a resistive cathode readout will be applied in the Mont-Blanc proton decay experiment[35].
- Limited geiger: the propagation of the geiger pulse along the sense wire is stopped by spacers[36] or nylon wires. The latter is applied in the PEP-4 (TPC) calorimeter.
- Analog readout: both methods may be combined with simple analog readout to further reduce pileup effects. The saturation limit may then be as high as about 15 GeV for electrons and more than 100 GeV for hadrons[37].

Other interesting developments go along the lines of applying the idea of track imaging to calorimeters.

Prototypes of a drift collection calorimeter have been tested by Price[38] and the principle of TPC has been applied to shower counters by Fischer and Ullaland[39] in the time-projection quanta-

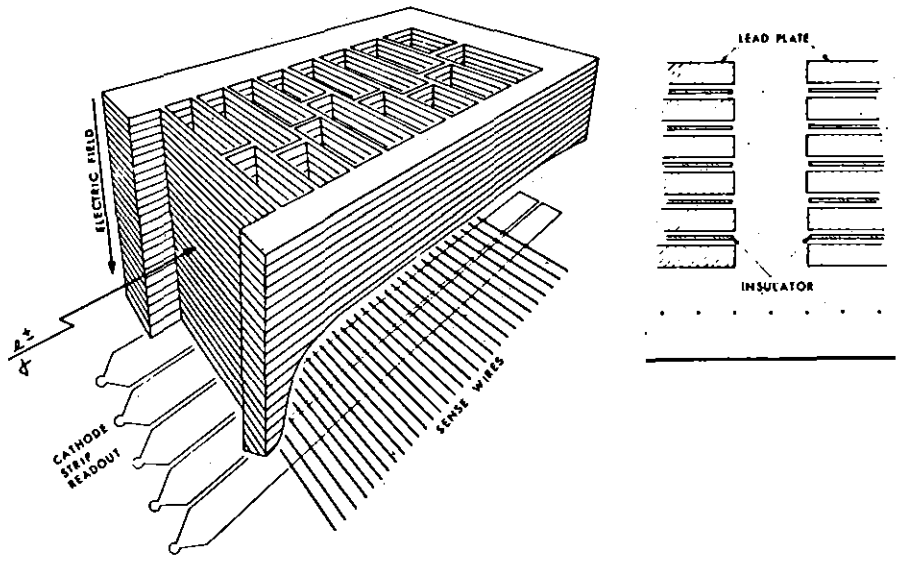


Fig. 4: Time projection quantameter of Fischer and Ullaland[39].

meter (Fig. 4) consisting of a TPC filled with material slabs allowing for shower development. Test results gave a linear response to the electron energy and a resolution of $\sigma_E/E = 33\%/\sqrt{E}$ was achieved.

## 4. Particle Identification

In all four techniques of particle identification (Table 4) attempts have been made in the last years to extend the range of applicability and/or increase the sensitivity and accuracy.

Table 4: Particle Identification

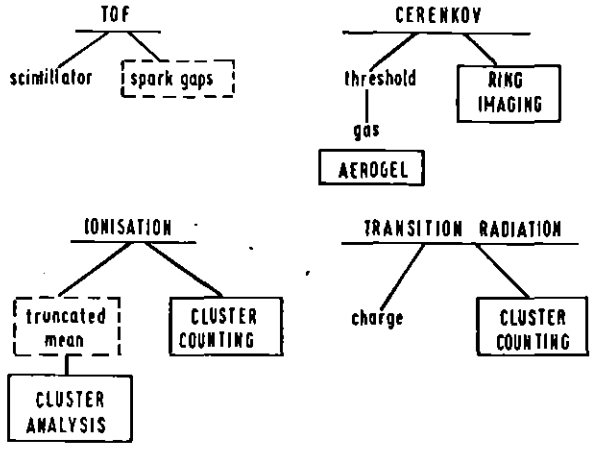

Time of flight

It has been proposed to use spark gaps instead of scintillation counters. In small test modules time resolutions of the order of 30 ps could be reached[56]. The feasibility of this method in large devices and a reliable long term performance still remain to be demonstrated.

Cerenkov counters

Threshold Cerenkov Counters

The fabrication of Silica Aerogel to fill the gap between TOF and liquid Cerenkov radiators on one side and gas Cerenkov on the other side has proven to be manageable[40]. Large quantities of Aerogel with refractive indices ranging from n = 1.02 to n = 1.05 were produced and employed in the AFS, EHS, EMC, and TASSO detector. To get full range identification with the available refractive indices however, high pressure counters have still to be added like in the AFS spectrometer.

An interesting idea for Cerenkov identification in a magnetic field has been applied in the HRS spectrometer (Fig. 5)[41]. Tori filled with high pressure gas are placed inside the solenoid field. The Cerenkov light is mirrored onto small photoionization chambers. The arrangement allows for K/π separation up to 4 GeV/c.

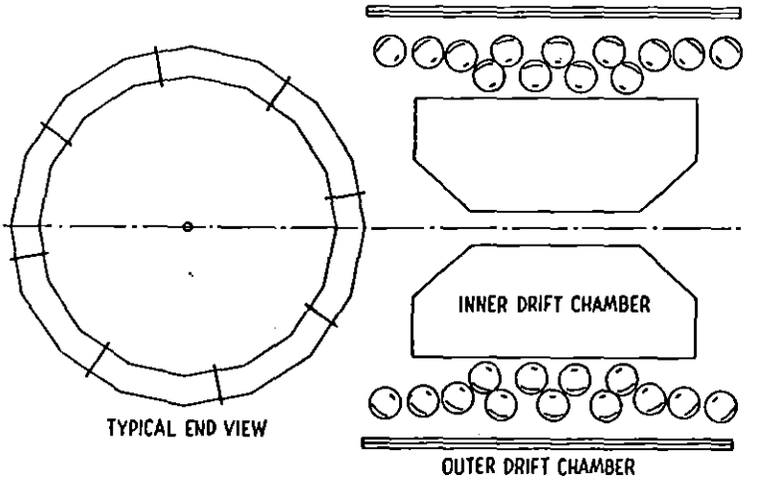


Fig. 5: Photoionization Cerenkov detector used in the High Resolution Spectrometer at PEP[41].

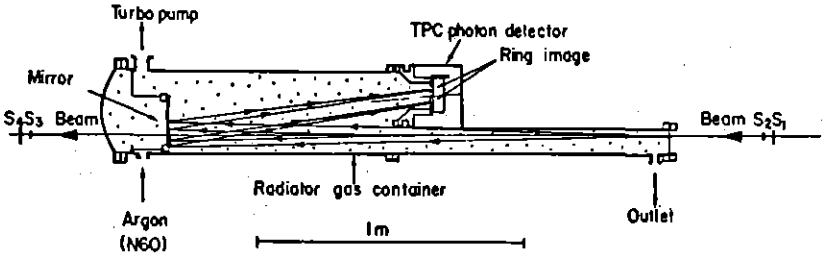


Fig. 6: Schematic Layout of the Cerenkov Ring image test detector used in Ref. 43.

Ring_Imaging_Cerenkov Counter

To overcome the limitations of threshold and differential counters in solid angle and granularity, the method of ring imaging was proposed[42]. The basically simple idea is illustrated in Fig. 6. A particle of velocity $\beta$ traversing a medium with refractive index $n > 1$ emits Cerenkov light at an angle $\theta = \arccos 1/\beta n$.

The light is focussed by a mirror of focal length L onto a plane where the ring image is detected. The radius R of the ring image is related to the particle velocity by

$$\frac{R}{L} \simeq \theta \simeq 1 - \frac{1}{\beta^2 n^2} = 1 - \gamma^2/n^2 \ (\gamma^2 - 1) \quad .$$

Three groups working on ring imaging prototypes are listed in table 5.

The CERN-Ecole Polytechnique-Uppsala group[43] uses a TPC type photon detector filled with methane and a few torr of photosensitive gas. Cerenkov light impinging through the chamber window releases photo-electrons. The ring image is drifted into a MWPC where it is detected. The latest tests were made with a radiator of 1.87 m Ar at STP. Using triethylamine (TEA) which is sensitive to photons with

Table 5: Cerenkov Ring Imaging Tests

| Group | Ref. | detector | radiator |
|---|---|---|---|
| CERN-Ecole Poly.-Upps. | 43 | TPC | Ar 1 and 2m |
| SLAC | 44 | multistep chamber | liquid He |
| CERN-Saclay-St. B. | 45 | - " _ | He 8m |

$E_\gamma \geq 7.5$ eV only and a $CaF_2$ window they got ring images with about 5 photoelectrons per event with 10GeV/c $\pi$'s. Recent tests with tetrakis-(diethylamine) ethylene (TMAE) which is sensitive to $E_\gamma \geq 5.4$ eV showed an increase to more than 9 photoelectrons per event. This in turn allowed to replace the window by quartz, which is transparent only below 7.5 eV but is less expensive and more stable. With TMAE and quartz they got 5.5 photoelectrons per event with 10 GeV/c $\pi$'s (specific detector response $N_o = 81\ cm^{-1}$), sufficient for ring image reconstruction. Fig. 7a shows an event detected with 10 GeV incident $\pi^-$ using TMAE and quartz windows. The resolution obtained so far is $\Delta\theta/\theta \simeq 3\%$. The aim is to improve this to 1.5%. Fig. 7b shows the $\pi$/e separation obtained at 7 GeV/c.

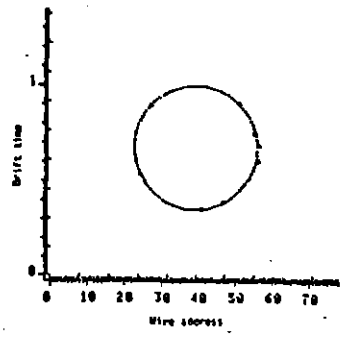

Fig. 7a

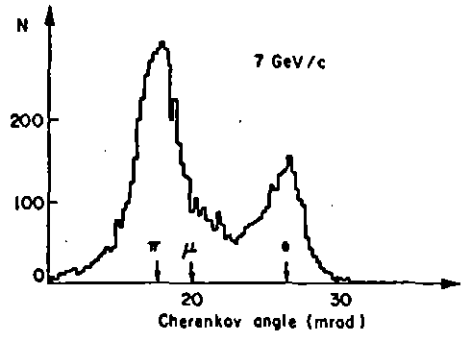


Fig. 7b

Fig. 7a: A ring image detected with a 1.87m Ar radiator using a fused quartz window and TMAE in the photon detector[43)]

7b: Angular distribution measured at 7 GeV showing clear peaks for $\pi$'s and e's and probably a small contribution from $\mu$'s between the two peaks.

The CERN-Saclay Stony Brook[45)] group is working with a multistep proportional chamber. TEA is used as photosensitive agent. Working with an 8 m long He radiator at STP they reached a sensitivity of 2.5 photoelectrons per event. Their resolution of $\Delta\theta/\theta \simeq 1\%$ allows for a clean separation of $\pi$/K/p at 200 GeV/c incident momentum (Fig. 8).

Ionization Measurement

Particle identification through specific ionization measurement is rather powerfull in the momentum range below the ionisation minimum. Fig. 9 shows as an example the results obtained in the CLEO detector[46)]. With a resolution of about 15% FWHM $\pi$/K/p are well separated.

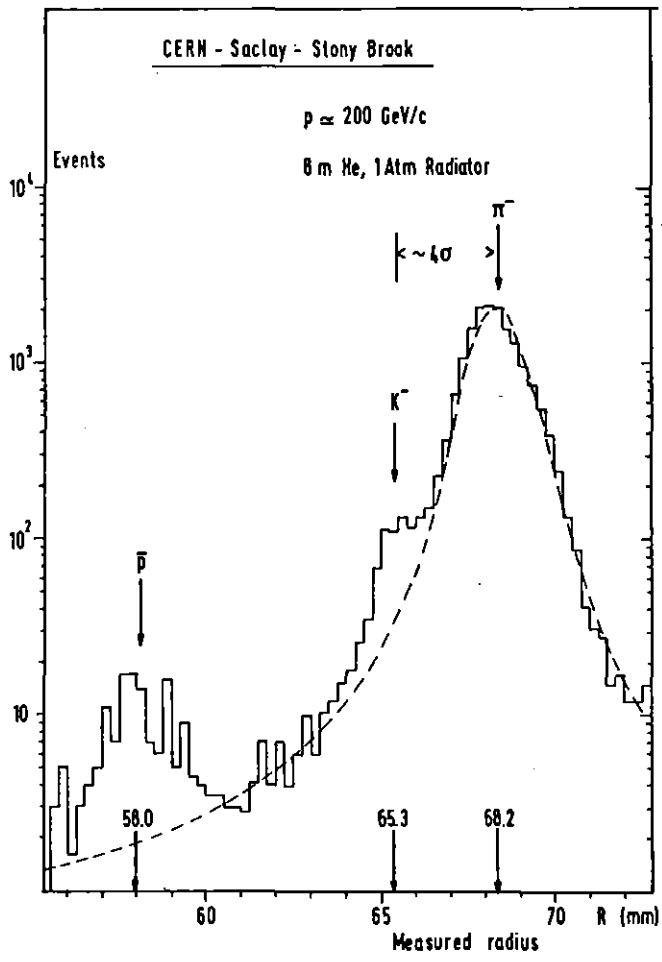


Fig. 8: Results obtained with an 8m He radiator in the test setup of Ref. 45. The resolution of 1% allows for good separation of $\bar{p}$, K and $\pi$ at 200 GeV/c incident momentum.

The task is much harder if one wants to extend the method to the region of the relativistic rise. A resolution of at least 7% FWHM is required to get full particle separation. To achieve this one has to suppress the Landau fluctuations ($\delta$-rays) due to large energy transfers in the primary processes. Usually one applies the "truncated mean", where many ionization samples are taken and only the lower measurements (typically 60%) are retained to calculate the average value. In table 6 several detectors are collected in which this method was recently applied (or will be applied).

A comparison between expectation and measurement shows that the resolution obtained in most large devices is worse than expected, even if the full tracklength is available for the measurement. To a large extent this is due to the difficulties in get-

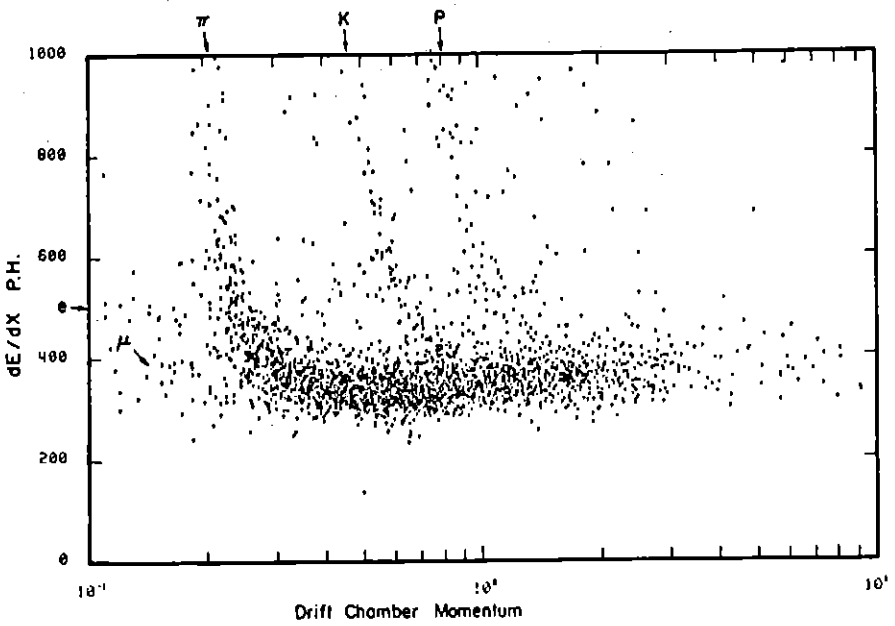


Fig. 9: Specific ionization (dE/dx) as a function of particle momentum as measured in the CLEO detector[46])

Table 6: $\frac{dE}{dx}$ resolution in some large devices

| Group | Ref. | Samples | Pressure (atm) | $\frac{dE}{dx}$ resolution (FWHM) expected | measured |
|---|---|---|---|---|---|
| EPI | 47 | 128 | 1 | 6% | 6-7% |
| ISIS 1 | 48 | 60-80 | 1 | 12±14% | 15±18% |
| JADE * | 5 | 48 | 4 | 10±11% | 13±14% |
| AFS | 10 | 42 | 1 | ∿21% | 24% |
| CLEO | 46 | 117 | 3 | 9.4% | 14% |
| ISIS 2 | 48 | 320 | 1 | 6% | |
| TPC | 17 | 185 | 10(7) | 5.5% | (6.5 test) |

*for $e^+e^-$; extrap. to pions: ∿15%; 10% test!

ting a good and stable calibration in big systems.

## Cluster Counting and Cluster Analysis

Investigations under way for further improvement go along two lines:

- Cluster Counting: To avoid Landau fluctuations, the primary ionization, which should follow a Poisson distribution, is counted by drifting the track through a "time expansion chamber" and subsequently detecting primary clusters in a proportional chamber.

Walenta and Rehak[49] found that the distribution of primary clusters is indeed Poisson like and the relativistic rise is compatible with the expectation taking into account diffusion effects. Further investigations under way indicate that the situation may be more complex[50].

- Cluster Analysis: In extension of the "truncated mean" method fine samplings are taken. The tracks are again drifted into a MWPC where very short time slices of down to 10 ns (corresponding to 0.25 mm) are analysed. Investigations by the BNL-City-Coll.[51] group show that the relativistic rise increases to more than a factor of 2 whereas the resolution deteriorates only slightly, resulting in a nearly two times better selectivity as one goes from 640 nsec (16 mm) to 10 ns (0.25 mm) sampling (Fig. 10). These results were confirmed in recent measurements with a more realistic test chamber having 10 layers of 2 × 2 cm drift space[52].

d) Transition Radiation

The transition radiation emitted by particles traversing dielectric discontinuities (e.g. Lithium foils or carbon foam) can be used for particle identification at very high momenta ($\gamma$ > few 100). The emitted UV light is usually detected in a proportional chamber placed behind the radiator. In this simplest configuration the pho-

Selectivity for p/e separation at 3.5 GeV/c

$$S = \frac{|E_p - E_e| - 2\sigma_e}{\sigma_p}$$

$E_{p,e}$ = truncated mean for p,e

$\sigma_{p,e}$ = stand. dev. of $E_{p,e}$

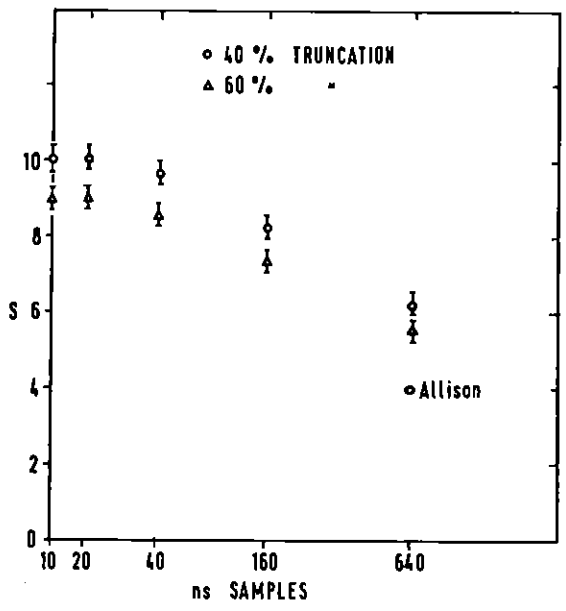


Fig. 10: Particle identification selectivity as a function of sample size extrapolated to 1m track length[51]

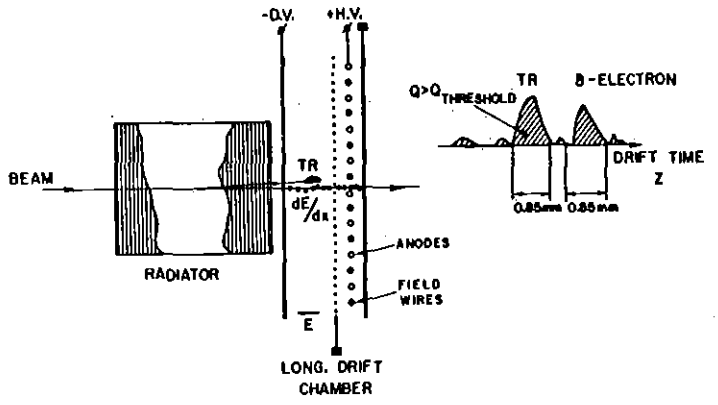


Fig. 11: Schematic illustration of the cluster counting method applied to transition radiation detection[53].

tonionization and the ionization of the charged particle cannot be separated. Several methods have been proposed to isolate the photon signal. One of the most promising attempts seems to be cluster counting[53]. Like in the corresponding case of ionization measurements described above the combined signal of transition radiation and dE/dx losses is detected in a drift region plus proportional chamber (Fig. 11). The signals are analysed similarly as in the case of cluster counting. With an appropriate setting of the threshold one can suppress most of the primary ionization of the track. Measurements showed a sensitivity 10 times better than with total charge integration[54]. Further tests are under way to check this result[55].

## Conclusions

We can draw the following conclusions

Track devices:

Although single wire resolution of $\leq$ 100 µm is reached in large cylindrical drift chambers, track resolution is still limited to about 200 µm due to various systematic uncertainties.

UV laser and X-ray calibration has been applied successfully in large setups and may further help to reduce some of the above uncertainties.

PEP - TPC has successfully been operated in cosmic rays.

Calorimetry:

BGO may be an interesting material for high resolution e/m calorimetry.

Wave length shifting has been successfully applied in large setups.

Scintillating fibres and photodiodes are being considered; feasibility in large calorimeters has still to be demonstrated.

A variety of gas calorimeters is on the market; limited streamer and geiger counters and high density imaging chambers offer interesting new aspects for large calorimeters.

Particle identification:

Aerogel is successfully operating in several detectors.

Cerenkov ring imaging has been proven to work in test setups. 5.5 photoelectrons have been detected with 10 GeV/c $\pi$'s and a 1.87m Ar radiator using a quartz window and TMAE in a photosensitive TPC.

$\frac{dE}{dx}$ ionization measurements for particle identification have been implemented in many large systems. Resolutions obtained so far are still worse than anticipated. Potential improvements by cluster counting and cluster analysis are being investigated. The cluster analysis seems to considerably increase the relativistic rise.

Cluster counting looks like an appropriate tool to increase sensitivity in transition radiation detectors.

Acknowledgement

I am indebted to T. Ekelöf, R. Kotthaus, and M. Albrow for critically reading the manuscript.

References

1) R.A. Eichler, contribution to this conference
M.A. Abolins, contribution to this conference

2) D. Aston, contribution to this conference

3) B. Schistad, contribution to this conference
L. Bugge, contribution to this conference

4) G. Bellini, invited talk at this conference

5) JADE Collaboration: W. Bartel et al., Phys.Lett. 88B (1979) 171
H. Drumm et al., Nucl.Instr. and Meth. 176 (1980) 333

6) TASSO Collaboration: R. Brandelik et al., Phys.Lett. 83B (1979) 261
H. Boerner et al., Nucl.Instr. and Meth. 176 (1980) 151

7) CELLO Collaboration: H.-J. Behrend et al., Phys.Scripta 23 (1981) 610

8) S. Stone, Phys. Scripta 23 (1981) 605

9) W. Davies-White et al., Nucl.Instr. and Meth. 160 (1979) 227

10) D. Cockerill et al., Phys. Scripta 23 (1981) 649

11) A.R. Clark et al., SLAC-PUB-5012 (1976)

12) C. Rubbia (Spokesman), CERN proposal SPSC/78-06 (1978) unpublished
B. Sadoulet, talk at the General Meeting on LEP, Villars (1981)

13) HRS proposal and J. Chapman, private communication

14) D. Hitlin, Phys.Scripta 23 (1981) 634

15) H. Hasemann et al., ARGUS Proposal, DESY F15/Pro 148 (1978) (unpublished)

16) J.E. Augustin et al., Phys. Scripta 23 (1981) 623

17) D. Fancher et al., Nucl.Instr. and Meth. 161 (1978) 38
D. Nygren, talk at the General Meeting on LEP, Villars (1981)

18) D. Bridges et al., Phys. Scripta 23 (1981) 655

19) J. Bourotte and B. Sadoulet, Nucl.Instr. and Meth. 173 (1980) 463

20) H.J. Hilke, Nucl.Instr. and Meth. 174 (1980) 145

21) H. Dietl, contribution to this conference

22) V.K. Bharadwaj et al. (presented by R.J. Morrison), contribution to this conference
V.K. Bharadwaj et al., Nucl.Instr. and Meth. 155 (1978) 411

23) H.A. Gordon, R.B. Palmer and S.D. Smith, Phys.Scripta 23(1981)564
H.A. Gordon and S.D. Smith, BNL 28380 (August 1980)

24) M. Martin, talk at the General Meeting on LEP, Villars (1981) and CERN SPSC/P147

25) S.R. Borenstein, R.B. Palmer, R.C. Strand, BNL 28546 and Phys. Scripta 23 (1981) 550

26) D. Perrin and P. Sonderegger, CERN OM/SPS/81-7

27) V. Eckardt et al., Nucl.Instr. and Meth. 155 (1978) 389

28) P.W. Jeffreys, contribution to this conference

29) W. Hofmann et al., (presented by J. Spengler), contribution to this conference

30) K. Pretzl, private communication

31) P. Slattery, contribution to this conference

32) A. Delfosse, O. Guisan, P. Mühlemann, Nucl.Instr. and Meth. 156 (1978) 425

33) M. Conversi and A. Gozzini, Nuovo Cim. 2 (1955) 189

34) G. Battistoni et al., Nucl.Instr. and Meth. 164 (1979) 57

35) G. Battistoni et al., Nucl.Instr. and Meth. 176 (1980) 297
E. Jarocci, contribution to this conference

36) E. Gygi and F. Schneider, CERN, EP Internal Report 80-08 (1980)

37) E. Jarocci, talk at the General Meeting on LEP, Villars (1981)

38) L.E. Price, Phys. Scripta 23 (1981) 685

39) H.G. Fischer and O. Ullaland, IEEE Trans.Nucl.Sci NS-27(1980)38

40) S. Hennig et al., Phys. Scripta 23 (1981) 697 and 703
P.J. Carlson et al., Phys. Scripta 23 (1981) 708
C. Arnault et al., Phys. Scripta 23 (1981) 710
P. Lecomte et al., Phys. Scripta 23 (1981) 376

41) J. Chapman, contribution to this conference

42) J. Séguinot and T. Ypsilantis, Nucl.Instr. and Meth. 142 (1977) 377

43) T. Ekelöf, contribution to this conference

44) R.S. Gilmore et al., SLAC-PUB-2629 (1980)

45) A. Peisert, talk at the General Meeting on LEP, Villars (1981)

46) A. Silvermann, talk at the General Meeting on LEP, Villars (1981)

47) I. Lehraus et al., Nucl.Instr. and Meth. 153 (1978) 347 and
Y. Goldschmidt-Clermont, private communication

48) W.W.M. Allison, talk at the General Meeting on LEP, Villars(1981)

49) P. Rehak and A.H. Walenta, IEEE Trans.Nucl.Sci. NS-27 (1980) 54

50) F. Piuz, private communication

51) T. Ludlam et al., IEEE Trans.Nucl.Sci. NS-28 (1981) 439
S.J. Lindenbaum, contribution to this conference

52) G. Jarlskog, talk at the General Meeting on LEP, Villars (1981)

53) T. Ludlam et al., Nucl.Instr. and Meth. (to be published)

54) C.W. Fabjan et al., CERN-EP/80-198 and Nucl.Instr. and Meth. (to be published)

55) M. Deutschmann, private communication

56) W. Braunschweig, Phys. Scripta 23 (1981) 383